

# A non-orthogonal material model of woven composites in the preforming process

<sup>a</sup>Weizhao Zhang<sup>#</sup>, <sup>a</sup>Huaqing Ren<sup>#</sup>, <sup>a</sup>Biao Liang, <sup>b</sup>Danielle Zeng, <sup>b</sup>Xuming Su, <sup>b</sup>Jeffrey Dahl, <sup>c</sup>Mansour Mirdamadi, <sup>d</sup>Qiangsheng Zhao, <sup>a</sup>Jian Cao (1)

<sup>a</sup>Department of Mechanical Engineering, Northwestern University, Evanston, IL, USA

<sup>b</sup>Ford Motor Company, Dearborn, MI, USA

<sup>c</sup>Dow Chemical Company, Midland, MI, USA

<sup>d</sup>Livermore Software Technology Corporation, Livermore, CA, USA

<sup>#</sup>Equal contribution

## 1. Introduction

Woven carbon fiber reinforced plastics (CFRPs) have received growing attentions from transportation industry because of their high performance to weight ratio [1, 2]. Due to its good geometric conformability, woven CFRP is most suitable for complex part geometries. A highly-automated process chain consisting of preforming and curing process developed recently to manufacture the CFRP parts at low cost and high speed. Materials used in the first preforming step is the stacked flat layers of prepregs, which are woven CFRPs impregnated with uncured thermoset resin in desired fiber orientations. These layers are heated above the resin melting temperature to fully soften the prepreg and formed into the part shape on a press. The formed part is then cured to harden the resin for the permanent shape [3].

There exists ample design freedom in woven CFRP products in terms of parameters or options in material design and preforming processes. The large consumption of the test material and the extensive experimental trial out period could lead to high developing cost and long product development cycle. Numerical methods that can simulate the preforming process should be developed in order to solve this problem [4].

A non-orthogonal model for the woven CFRP preforming process is developed in this work, which has been incorporated into the LS-DYNA<sup>®</sup> software as MAT\_293 (MAT\_COMPFRF) through the joint effort of this academic and industry team. Following in this paper is the detailed illustration of the fundamentals of this model and its experimental validation conducted at an industrial lab. Additionally, the measurement of interaction between prepreg layers is also characterized.

## 2. Analysis of the material deformation mechanism

Woven CFRPs are highly anisotropic in mechanical properties. The prepreg has large tensile modulus along the warp and weft yarn directions because of the stiff carbon fibers, but small intra-ply shear modulus, especially at the preforming temperature when the resin is molten as the shear resistance is mostly provided by the resin and the friction between the fiber yarns. During the preforming, the most dominant deformation mode is the intra-ply shear. To capture this mechanism, we propose to fully decouple the tension and shear deformation and the decoupling must hold well under large shear deformation.

Stress analysis for the woven CFRP with the modified non-orthogonal model is shown in Fig. 1.  $\sigma_{f1}$  and  $\sigma_{f2}$  are the stress components caused by yarn stretch, and they are along the warp and weft yarn directions, respectively.  $\sigma_{m1}$  and  $\sigma_{m2}$  are the stress components caused by the yarn rotation. These stress components will be transformed into the local corotational coordinate, summed up as  $\sigma_{xx}$ ,  $\sigma_{xy}$ , and  $\sigma_{yy}$ , and will be the stress outputs reported from the material model to the FEM software.

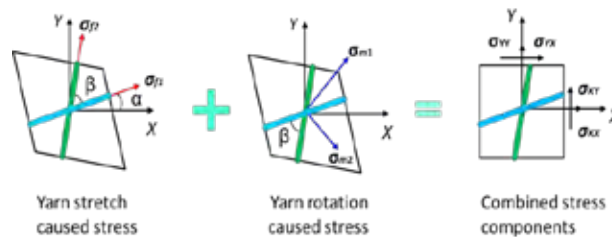


Fig. 1. Stress analysis of the woven CFRP with the modified non-orthogonal model.

The deformation gradient tensor  $\mathbf{F}$  is utilized in this model to trace the yarn directions and stretch ratios during the preforming via  $\mathbf{g} = \mathbf{F} \cdot \mathbf{G}$ , where  $\mathbf{g}$  and  $\mathbf{G}$  are the final and initial orientations of the local fibers respectively. It can be used to calculate  $\alpha$ , which indicates the relative rotation between the local warp direction and the  $X$ -direction in the local corotational coordinate, and yarn angle  $\beta$ , which indicates the amount of shear deformation in the material.

The model was implemented into the FEM software LS-DYNA<sup>®</sup> as MAT\_293 (MAT\_COMPFRF). MAT\_293 enables users to directly input experimental data to define the stress-strain curves, as well as the shear locking angle, which indicates whether the shear deformation reaches to the extent that the rotation resistance between warp and weft yarns is no longer small compared to the tensile modulus of the material. The flowchart of the model is shown in Fig. 2.

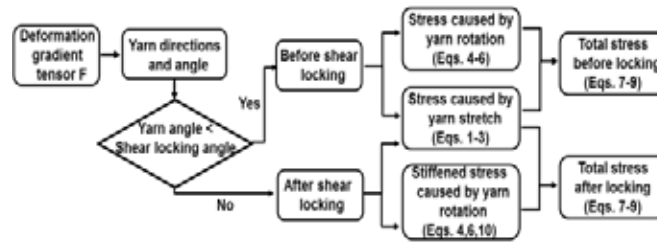


Fig. 2. Calculation flowchart of the LS-DYNA MAT\_293.

In the material subroutine, the warp and weft directions for each element are calculated from the deformation gradient tensor. If the angle between the warp and weft yarns are smaller than the shear locking angle, then the small shear modulus condition will hold. If the angle between the warp and weft yarns reaches to the shear locking angle, the resistance for further shear deformation will greatly increase because the contacted fiber yarns stiffen the woven structure. In this situation, the shear resistance of the model will increase automatically to avoid further large shear deformation.

**3. Material characterization**

Material characterization is essential for the FEM model to predict the behavior of the woven CFRPs during the preforming process. It can be seen from Fig. 1 that the stresses caused by both yarn stretch and yarn rotation need to be calibrated for any specific woven material that is of interest. The calibration can be performed experimentally by the uniaxial tension and bias-extension tests [5]. The undulation strain and the stable tensile modulus along the yarn directions, as shown in Fig. 3(a), are obtained from the uniaxial tension test. In the FEM calculation, at every material point, once the stretch ratio along the yarns was obtained from the deformation gradient tensor, the resulting stress due to yarn stretch, i.e., “yarn stretch caused stress”  $\sigma_{f1}$  and  $\sigma_{f2}$ , can be obtained by referencing to the data in Fig. 3 (a). The shear behavior obtained via the bias-extension test, as shown in Fig. 3(b), is directly implemented as a polynomial function into the model to calculate the “yarn rotation caused stress”  $\sigma_{m1}$  and  $\sigma_{m2}$  given the angle change between the warp and weft yarns obtained from the deformation gradient tensor. The shear locking angle is also measured after the test and input to the model for the small/large shear moduli selection process shown in Fig. 2.

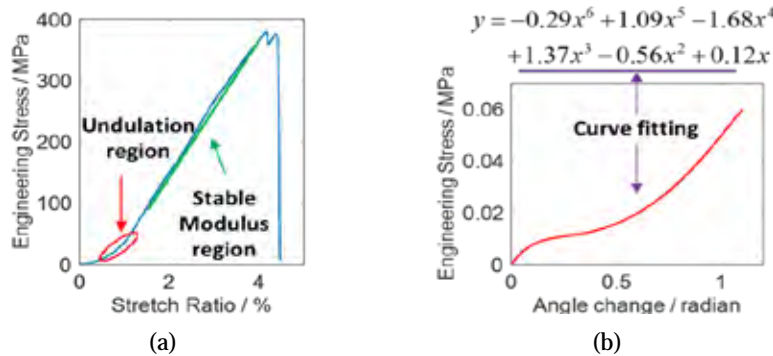


Fig. 3. (a) Uniaxial tension test result for undulation and tensile modulus characterization and (b) bias-extension test result for shear deformation characterization

However, these two tests only provide the in-plane intra-ply properties of the material. During the preforming simulation, the bending behavior of the single layer and the interaction between the composite layers will also affect the in-plane strain distribution and the wrinkling initiation. Hence, characterizations of bending stiffness and inter-ply interaction are also necessary.

Bending stiffness of the composite is characterized with the cantilever beam system, as shown in Fig. 4(a). During the test, the single-ply prepreg will deform under gravity and the deflection is measured by a digital image analysis system. A bending test simulation model is utilized for parameter calibration. Material properties such as tensile modulus and composite density are inputs to the FEM model. Then the compressive modulus is adjusted until the same displacement in the Y direction of the end tip as that in the experiment is achieved. The final bending profile will be compared as shown in Fig. 4(b) to confirm the approach.

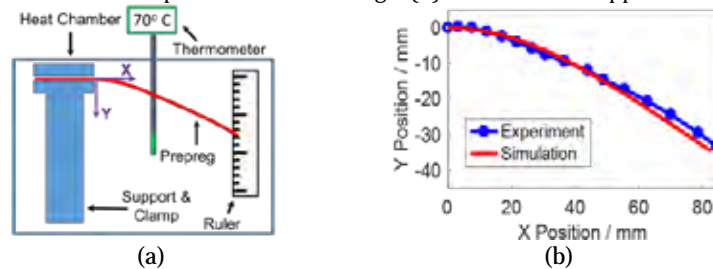


Fig. 4. (a) Experimental setup, and (b) bending shape comparison at 70°C for bending stiffness characterization.

The setup for interaction characterization is demonstrated in Fig. 5(a). It moves two prepreg layers relative to each other for the interaction characterization. A load cell records the normal and horizontal forces, whose ratio is defined as the interaction factor. One example of the histories of forces and the interaction factor in a test is shown in Fig. 5(b), while the stable value of the interaction factor

is used in FEM. The preforming process operates at the temperature ranging from 60°C to 80°C, and the characterization results at different temperatures, sliding speeds, and fiber yarn orientations are shown in Fig. 6.

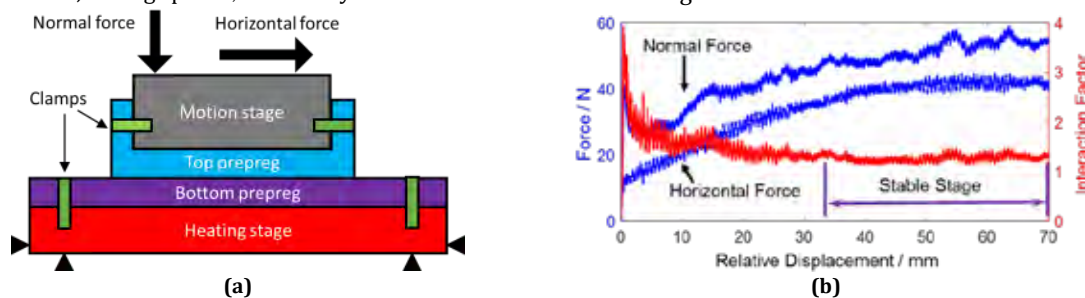


Fig. 5. (a) Experimental setup for the interaction characterization, and (b) force and interaction factor history at 5 mm/s, 70°C, 0 degree yarn angle difference

It can be seen in Fig. 6 that when the temperature is fixed, the interaction factors at various sliding speeds and fiber orientations do not change significantly. For convenience, in one preforming simulation, assuming that the temperature distribution is uniform, the interaction factor will be treated as a constant.

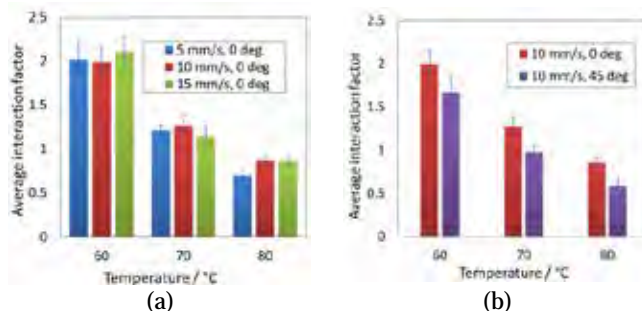


Fig. 6. Interaction factor at various temperatures subjected to different (a) relative motion speeds and (b) fiber yarn orientations.

#### 4. Experimental validation

The double-dome test, as shown in Fig. 7, was conducted and simulated to demonstrate the capability of the material model for 3D shape forming regarding different yarn orientations and stacking sequences. The simulation model was established in LS-DYNA® using the explicit integration method. The sheet was modeled by reduced integrated shell elements. Each element is about 4 mm × 4 mm with five through-thickness integration points. The punch, binder and die were modeled by rigid shell elements.



Fig. 7. Experimental setup for the double dome test.

The simulation results in the upper-right quarter of Fig. 8 shows that the non-orthogonal material model established is capable of accurately predicting the physical experiments regarding the yarn angle distribution and blank draw-ins. For instance, the deviation of the maximum draw-in distance is about 7 mm (49 mm in experiment versus 42 mm in simulation). For comparison, an orthotropic material model (MAT\_002) is utilized in another simulation whose result is shown in the upper-left quarter of Fig. 8 in the same scale as non-orthogonal model and experiment results. Since the orthotropic model cannot track the material property change during the yarns' rotation, the corresponding simulation has a maximum draw-in deviation of 24 mm, not capturing the overall process behavior.

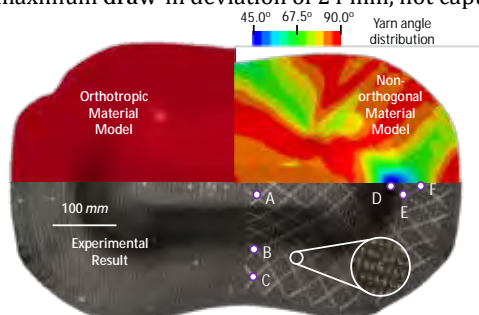


Fig. 8. Simulation and experimental results comparison of deformed geometry and yarn angle distribution for double dome preformed part of ±45° single layer woven prepreg.

In the non-orthogonal model, the yarn angle is defined as an output variable, while MAT\_002 does not have the capability for direct visualization. For clarity, Table 1 compares the resulting shear angles at various locations obtained from the experiment and simulations. Again, it shows that the current model has improved the prediction accuracy.

**Table 1** Resulting yarn angles from the single-layer case

Location	A	B	C	D	E	F
Experiment	80°	88°	71°	49°	56°	66°
Sim-orthotropic	70°	85°	86°	47°	59°	77°
Sim-present	81°	88°	73°	46°	60°	70°

The double-layer preforming test was conducted next. These two blanks were modeled by two layers of shell elements with different initial yarn orientations. The inter-ply interaction was simulated via the Coulomb friction model. The experimental and simulation results are shown in Fig. 9 from both top and bottom views, with both part geometry and wrinkle location marked. The simulation predicts the overall geometry and relative motion of two prepreg sheets well. The slight discrepancy might be caused by the constant interaction factor in the simulation, while in reality, it might be velocity- and pressure-dependent. Furthermore, the thickness distribution due to deformation will not be uniform, which may influence the frictional interaction and need to be captured by advanced shell elements or continuum elements.

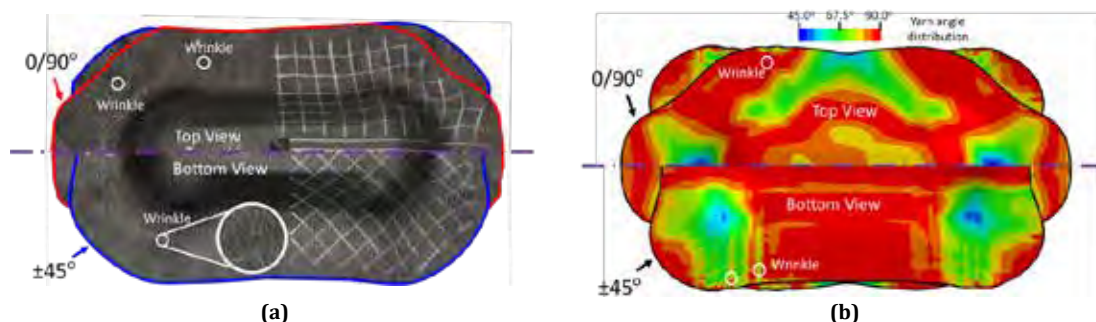


Fig. 9. Double dome preformed part of double-layer woven prepregs (a) experimental result, (b) simulation result.

## 5. Conclusions

An improved non-orthogonal material model that decouples the tension and shear behavior of the woven CFRPs under large shear deformation is proposed and implemented in the commercial finite element software LS-DYNA® for the composite preforming process. A systematic set of material characterization methods are developed to characterize both intra and inter-ply properties. With calibrated material properties, the material model can accurately predict the 3D deformation of the woven CFRP prepregs in preforming, demonstrated by the comparison between the simulation and experimental results from a double dome study.

## Acknowledgements

This work was supported by the Office of Energy Efficiency and Renewable Energy (EERE), U.S. Department of Energy, under Award Number DE-EE0006867.

## References

- [1] Teti R. Machining of Composite Materials. *CIRP Annals - Manufacturing Technology*. 2002;51(2):611-34.
- [2] Brinksmeier E, Janssen R. Drilling of Multi-Layer Composite Materials consisting of Carbon Fiber Reinforced Plastics (CFRP), Titanium and Aluminum Alloys. *CIRP Annals - Manufacturing Technology*. 2002;51(1):87-90.
- [3] Yanagimoto J, Ikeuchi K. Sheet forming process of carbon fiber reinforced plastics for lightweight parts. *CIRP Annals - Manufacturing Technology*. 2012;61(1):247-50.
- [4] Hamila N, Boisse P, Sabourin F, Brunet M. A semi-discrete shell finite element for textile composite reinforcement forming simulation. *International Journal for Numerical Methods in Engineering*. 2009;79(12):1443-66.
- [5] Cao J, Akkerman R, Boisse P, Chen J, Cheng HS, de Graaf EF, Gorczyca JL, Harrison P, Hivet G, Launay J, Lee W, Liu L, Lomov SV, Long A, de Luyccker E, Morestin F, Padvoiskis J, Peng XQ, Sherwood J, Stoilova T, Tao XM, Verpoest I, Willems A, Wiggers J, Yu TX, Zhu B. Characterization of mechanical behavior of woven fabrics: Experimental methods and benchmark results. *Composites Part A: Applied Science and Manufacturing*. 2008;39(6):1037-53.